Photoluminescence of nanocrystals embedded in oxide matrices

C. Estrada, J.A. Gonzalez, A. Kunold
Ciencias Básicas, UAM-Azcapotzalco, Av. S. Pablo 180, C. P. 02200, México D. F., México.
email akb@correo.azc.uam.mx

J. A Reyes-Esqueda
Instituto de Física, UNAM, México D. F., México

P.Pereyra
Ciencias Básicas, UAM-Azcapotzalco, Av. S. Pablo 180, C. P. 02200, México D. F., México.

We used the theory of finite periodic systems to explain the photoluminescence spectra dependence on the average diameter of nanocrystals embedded in oxide matrices. Because of the broad matrix band gap, the photoluminescence response is basically determined by isolated nanocrystals and sequences of a few of them. With this model we were able to reproduce the shape and displacement of the experimentally observed photoluminescence spectra.

I. INTRODUCTION

ZnO-Ge and SiO2-Ge nanocomposites are intensively studied for their possible use as optoelectronic devices[1,2,3,4,5]. A common method for preparing these systems is by alternate deposition of oxides and Ge, followed by an annealing process to increase the diffusion of nanocrystalites (NC) into the adjacent layers[4,6,7,8,9]. This process leads also to homogenize the sizes and spacial dispersion of NCs. It is widely known that the photoluminescense-spectra shift is strongly related to NC's size. Although there have been several attempts to understand the relation between the morphology and the photoluminescence (PL) response of embedded NC in oxide matrices[1,4,6], none of them lead to a simple and precise explanation. The purpose of this work is to understand and to explain this relation from a simple model and a few physical parameters.

To calculate the optical response of these rather complex systems, we use both the *bona fide* multiple-quantum-well electron and hole eigenvalues and eigenfunctions, obtained from the theory of finite periodical systems[10] (TFPS) and a simple assumption, experimentally supported, on the statistical distributions of NC sizes. We show that the main features of the PL spectra (in Ref.[1] for Ge doped ZnO films annealed at several temperatures), can clearly be identified in terms of the interband excitonic transitions calculated for multiple quantum well (MQW) systems, whose well and barrier parameters are drawn from the experimental system. The agreement with other kind of experimental results, as those reported by by S. Takeoka et al.[4] for Ge NC in SiO_2, is also good when the nanocrystals-size dispersion is taken into account.

II. THE MODEL

In Fig. 1 we observe micrographs of Ge cristalites embedded in a ZnO matrix. At low NC densities we have almost isolated NCs (see Fig 1 (a)), while at higher NC densities one can find groups of NCs aligned and almost equidistant(see Fig. 1 (b)). Although a single NC can be better modeled as a quantum dot, the relevance of the longitudinal coherence in the energy spectra of a sequence of NCs, leads us to model the sequence as a multiple

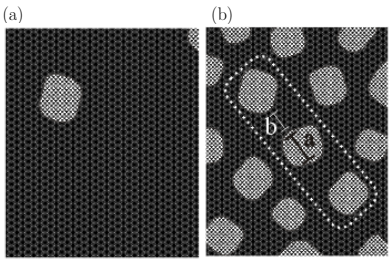

FIG. 1: Ge cristalites embedded in a ZnO matrix for (a) low NCs densities and (b) high densities.

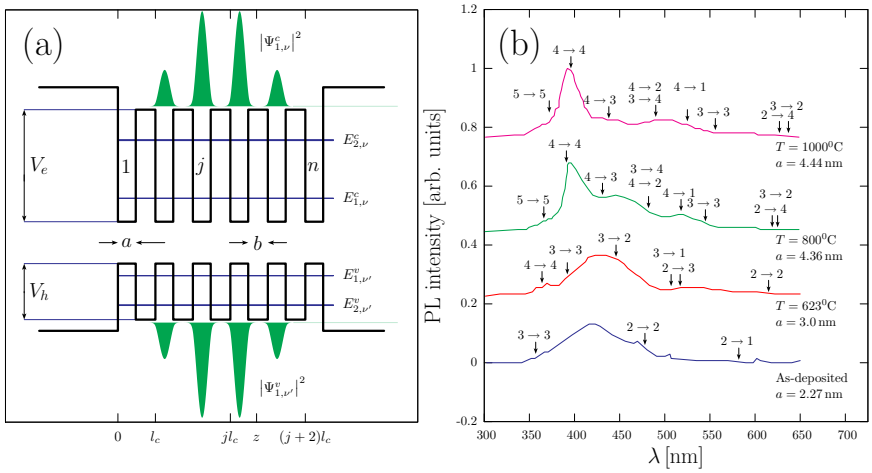

FIG. 2: (a) Finite periodic square-well modulation of the valence and conduction band edges along a set of n QW's. Also we show the wave functions $\Psi^c_{1,1}$ and $\Psi^v_{1,1}$ for the first energy level of the first subband in the conduction and valence band. For these wave functions the electron and hole are localized inside the QW's. (b) Room temperature PL spectra of Ge doped ZnO films annealed at several temperatures and theoretical peaks position (black arrows). We also show the corresponding NC's average diameter used for the theoretical model.

1D-quantum well potential. Each of these sequences is then treated as a finite periodic square-well potential (see Fig. 2 (a)), and the whole nanocomposite PL response results from the contribution of an ensemble of MQWs, which differ basically in the number of NCs, well-widths and barrier-thicknesses.

In Fig. 2 (a) we have a MQW potential for a given set of parameters. We show the energy spectra (in the conduction and valence bands), and the square of the wave function amplitude $\psi^{c(v)}_{1,1}$ for the first energy level in the first conduction (valence) subband. In the TFPS, these quantities can easily be calculated. The eigenvalues are obtained from[10]

$$(\alpha_n e^{ika} - \alpha^*_n e^{-ika}) + \beta_n - \beta^*_n = 0, \tag{1}$$

with $k = \sqrt{2mE/\hbar^2}$ and m the electron or hole effective mass. The wave functions at any point z in the $(j+1)$-th cell (for a system of length $L = nl_c$) and energy E are given by

$$\Psi^\iota(z,E) = A[(\alpha_p + \gamma_p)(\alpha_j - \beta_j \frac{\alpha_n + \beta^*_n}{\alpha^*_n + \beta_n}) + (\beta_p + \delta_p)(\beta^*_j - \alpha_j \frac{\alpha_n + \beta^*_n}{\alpha^*_n + \beta_n})]. \tag{2}$$

α_j, β_j are elements of the transfer matrix $M(jl_c, 0; E)$ and $\alpha_p, \beta_p, \gamma_p, \delta_p$ are elements of a partial cell transfer matrix $M_p(z, jl_c; E)$. $\Psi^\iota(z, E^\iota_{\mu,\nu})$ (with $\iota = c, v$ for conduction and valence bands), is the eigenfunction corresponding to the eigenvalue $E^\iota_{\mu,\nu}$. To evaluate the PL response we use the following function

$$\chi = \sum_{\nu,\nu',\mu,\mu'} \frac{p_{\nu,\nu',\mu,\mu'} f\left(E^c_{\mu,\nu}\right)\left[1 - f\left(E^v_{\mu',\nu'}\right)\right]}{(w_s - E^c_{\mu\nu} + E^v_{\mu'\nu'})^2 + \Gamma^2}. \tag{3}$$

$f(E^\iota_{\mu,\nu})$ the Fermi-Dirac carrier distribution functions in the conduction or valence band.

III. RESULTS AND DISCUSSION.

In Fig. 2 (b) we present the experimental PL spectra of Ge-doped ZnO films for different annealing temperatures, reported in Ref.[1]. The NC's average diameter increases with the annealing temperature[8]. The peaks position in these PL curves can be described in terms of the energy spectra of a single sequence of NCs. For this calculation we use the potential and gap parameters corresponding to the Γ point of ZnO and the annealing temperature, i.e. $m^e_{Ge} = 0.12m_e$, $m^h_{Ge} = 0.23m_e$, $m^e_{ZnO} = 0.24m_e$, $m^h_{ZnO} = 0.45m_e$, $E_{Ge} = 0.66$eV,$E_{ZnO} = 3.31$eV. The black arrows point out the theoretical predictions for different possible recombination transitions. In this figure, the assignment $\mu \rightarrow \mu$ refers to the energy transitions $E^c_{\mu,\nu} \rightarrow E^v_{\mu,\nu}$. It is well known that increasing the well width a, the subbands move towards lower energies while their number increases. We notice in the the experimental PL curves that increasing a the small

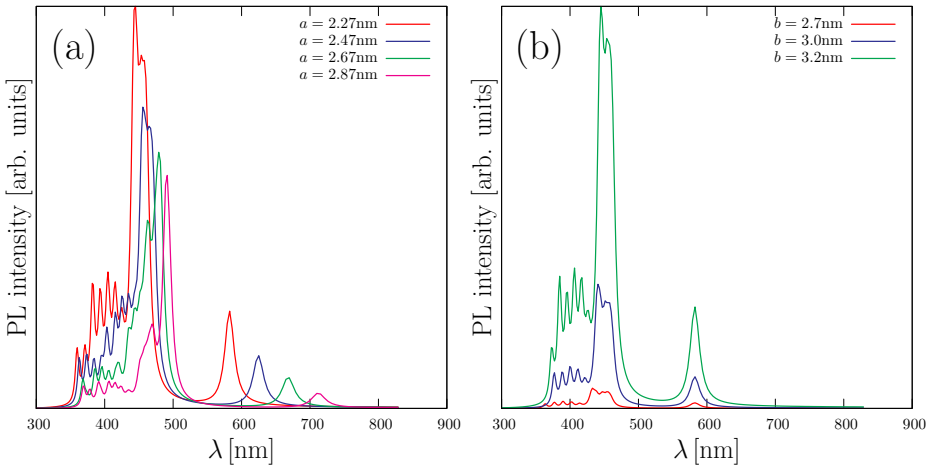

FIG. 3: Theoretical PL spectra of Ge doped ZnO films for (a) several NCs diameters and (b) barrier widths.

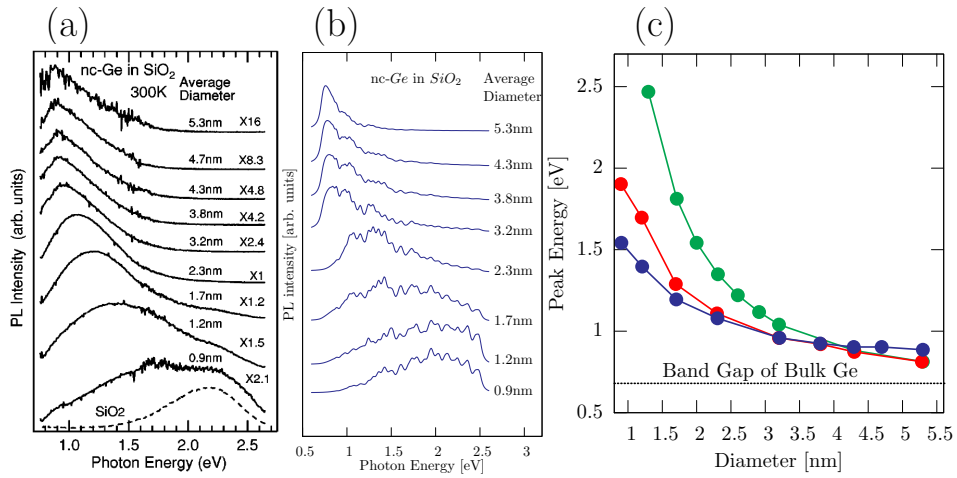

FIG. 4: At the left the measured PL response for different average diameters of NC-Ge embedded in SiO_2. In the middle our theoretical curves, and at the right image we plot the PL peak energy versus average diameter of NC-Ge for: experiment[4], the theoretical prediction with size-dispersion and without size-dispersion.

peaks shift toward larger wave lengths, while the main PL peak displaces in the opposite direction. This behavior is even much clear in the experimental results of Takeoka eta al. in Ref.[4], where the secondary-peaks structure is absent.

In these systems the experimental curves arise from the contribution of a large number of NCs which sizes are statistically distributed[8]. The PL aspect and peaks relative-height depend not only on the potential parameters, but also on their statical distribution. The PL response of a single MQW in Fig. 3, shows the red-shift with a and the high PL sensitivity to small barrier-thickness variations.

To explain the experimental results reported by Takeoka et al. in Ref[4] for Ge Ncs in a $Si0_2$ matrix, we need to take into account also the NC's size distribution. We assume, according with the experimental results, that the size distribution is described by a log-normal function. We then calculate the PL spectra of several sets of NC diameters, pondered by their statistical weight. Since the PL peaks position is less sensitive to the number of wells and to the NC spacing, we assume for this case a fixed barrier width and also a fixed number of cells.

At Fig. 4 (a) we present the experimental results from Ref.[4]. In Fig. 4 (b) we show our calculated curves assuming up to 50 contributing MQW sequences with the following parameters: $m^e_{SiO_2} = 0.5m_e$, $m^h_{SiO_2} = 0.49m_e$,$E_{SiO_2} = 9.3$eV, corresponding also to the Γ point of SiO_2. At Fig. 4 (c), we plot also the peak position versus the NCs average diameter. This averaging procedure improves the agreement with the experimental PL spectra. The size-dispersion shifts the PL peaks toward lower energies. This is a consequence of the asymmetry of the log-normal distribution.

In our calculation we neglected e-h Coulomb interaction corrections. In any case, they will produce small red shifts in the secondary PL peak positions and will be washed out in the main peak behavior.

IV. CONCLUSIONS

To explain the photoluminescence response of NCs embedded in oxide matrices as function of the average NCs diameter, we modeled these systems as a collection of 1-D multiple-quantum-well potentials. Using the finite periodical systems theory and a simple NC-size distributions assumption, we shown that the calculated 1-D MQW subband transitions, describe correctly the secondary PL peaks behavior, observed by Fan et al.[1], as function of the NCs diameter. We have shown also that the main PL peak blue-shift behavior, observed by Takeoka et al. in Ref.[4], is basically determined by the statistical dispersion of the NCs diameter.

[1] D.H. Fan, Z.Y. Ning, and M.F. Jiang, Appl. Surface Science **245**, 414 (2005).
[2] B.J. Jin, S. Im, and S.Y. Lee, Thin Solid Films **366**, 107 (2000).
[3] D.M. Bagnall, Y.F. Chen, Z. Zhu, T. Yao, S. Koyama, M.Y. Shen, and T. Goto, Appl. phys. Lett. **70**, 2230 (1997).
[4] S. Takeoka, M. Fujii, S. Hayashi, and K. Yamamoto, Phys. Rev. B **58**, 7921, (1998).
[5] B. Chu, D. Fan, W.L. Li, Z.R. Hong, and R.G. Li, Appl. Phys. Lett. **81**,10 (2002).
[6] Y. Maeda, N. Tsukamoto, Y. Yazawa, Y. Kanemitsu, and Y. Masumoto, Appl. Phys. Lett. **59**, 3168 (1991).
[7] Y. Kanemitsu, H. Uto, Y. Masumoto, and Y. Maeda, Appl. Phys. Lett. **61**, 2187 (1992).
[8] Y. Maeda, Phys. Rev. B **51**, 1658 (1995).
[9] S. Okamoto, and Y. Kanemitsu, Phys. Rev. B **54**, 16421 (1996).
[10] P. Pereyra, Annals of Physics **320**, 1 (2005).